Reprinted from Journal of the Optical Society of America B, Vol. 2, p. 407, March 1985

Isoelectronic studies of the $4s4p\ ^3P_J$ energy levels in the Zn sequence

Lorenzo J. Curtis

Department of Physics and Astronomy, University of Toledo, Toledo, Ohio 43606

Received July 27, 1984; accepted November 19, 1984

Screening parameterizations of the spin–orbit and exchange energies are used to systematize available data accurately for the $4s4p$ configuration in the Zn isoelectronic sequence. Through the availability of precision measurements of the $4s^2\ ^1S_0$–$4s4p\ ^1P_1$ resonance transition, these screening parameterizations are used to make accurate interpolative and extrapolative predictions of the excitation energies of the $4s4p\ ^3P_J$ levels for ions from Ge III through Ba XXVII. These results also provide extrapolative predictions of the magnetic-dipole, electric-quadrupole, and intercombination transitions in this system that sometimes occur in localized diagnostics of high-temperature plasmas.

INTRODUCTION

The first excited configuration of the Zn isoelectronic sequence has recently been the object of a number of experimental studies utilizing laser-produced plasma,[1,2] beam-foil,[3,4] and tokamak plasma[5,6] excitation methods. Accurate predictions of the $4s4p\ ^3P_J$ excitation energies for highly ionized members of this sequence would be valuable because spin-intercombination and intraterm transitions from them become relatively stronger with increasing nuclear charge and can be observed in high-temperature plasmas when heavy elements are present as impurities or as diagnostic probes. Theoretical calculations of the resonance and intercombination lines have been made,[7,8] but these predictions differ from observed values typically by several percent and are not of sufficient accuracy to facilitate spectroscopic classification.

A screening parameter method[9] was developed earlier with application to the Mg sequence, which permits reliable semiempirical predictions of the positions of the triplet levels relative to the singlet level for an $nsnp$ configuration. Observations for the $4s4p\ ^1P_1$ excitation energy to high stages of ionization are now available,[1] and we present here a semiempirical parameterization of the available data base to interpolate and extrapolate accurately the $4s4p\ ^3P_J$ excitation energies in the Zn sequence.

REDUCTION AND PARAMETERIZATION OF THE MEASURED DATA

The semiempirical parameterization used here involves only a slight generalization of that described in detail in Ref. 9. It utilizes the Slater intermediate coupling formulas that relate the excitation energies (denoted here by their spectroscopic symbols) to the interelectron electrostatic energies and magnetic splitting factors in a pure sp configuration [Eq. (16.1) of Ref. 10]. When used to describe differences between the singlet and triplet excitation energies $^1P_1$–^3P_J, these formulas involve only two quantities, the spin–orbit energy ζ and the exchange Slater energy G_1. If the observed excitation energies are converted to effective values for ζ and G_1, these secondary quantities often exhibit a simpler scaling with nuclear charge than do the raw data, and linear interpolation and extrapolation schemes can be developed using screening parameterizations.

The modification of the method described in Ref. 9 that was adopted here involves the fact that ζ and G_1 are overdetermined and can be deduced from the three-triplet energy differences in a number of ways. Various perturbations (deviations from the single-configuration assumption, spin–spin and spin–other-orbit interactions, etc.) can cause a breakdown of the exact validity of the equations. Thus the values of ζ and G_1 can depend slightly on the method of calculation, and a recomputation of the triplet energies can lack complete reciprocity. For the Mg sequence these discrepancies are generally smaller than the experimental uncertainties, but for the more complex Zn sequence they can be sufficiently large to warrant consideration. Our purpose here is to parameterize the data accurately and not to ascribe physical validity to the model, and the overdeterminacy can be removed simply by defining a third quantity. Thus a quantity G_{1A} was defined exclusive of the $^3P_1$ level, and another quantity G_{1B} was defined involving $^3P_0$ and $^3P_2$ only through ζ, ensuring uniqueness and reciprocity between the measured intervals and reduced quantities. The parameterization was carried out in terms of three intervals, which have the following relationships to G_1 and ζ:

$$A \equiv {}^1P_1\text{–}{}^3P_2 = G_{1A} - 3\zeta/4 + [(G_{1A} + \zeta/4)^2 + \zeta^2/2]^{1/2}, \quad (1)$$

$$B \equiv {}^1P_1\text{–}{}^3P_1 = 2[(G_{1B} + \zeta/4)^2 + \zeta^2/2]^{1/2}, \quad (2)$$

$$C \equiv {}^3P_2\text{–}{}^3P_0 = 3\zeta/2. \quad (3)$$

These can be inverted to yield

$$\zeta = 2C/3, \quad (4)$$

$$G_{1A} = A(A + 3\zeta/2)/2(A + \zeta), \quad (5)$$

$$G_{1B} = (B^2 - 2\zeta^2)^{1/2}/2 - \zeta/4. \quad (6)$$

0740-3224/85/030407-04$02.00

Table 1. Observed and Predicted Energy Levels for the $4s4p\ ^3P$ Terms in the Zn Isoelectronic Sequence (in cm^{-1})

Z	Ion	$^1P_1$ (Obs.)	$^3P_0$		$^3P_1$		$^3P_2$		Source
			Obs.	Pred.	Obs.	Pred.	Obs.	Pred.	
30	Zn I	46 745[a]	32 311[a]	–	32 501[a]	–	32 890[a]	–	Ref. 12
31	Ga II	70 700[a]	47 370[a]	–	47 816[a]	–	48 750[a]	–	Ref. 13
32	Ge III	91 873(4)[b]	61 733(6)[b]	61 823	62 496(2)[b]	62 518	64 138(6)[b]	64 145	Ref. 14
33	As IV	112 022(6)[b]	75 812(7)[b]	75 793	76 962(3)[b]	76 899	79 492(7)[b]	79 466	Refs. 15, 17
34	Se V	131 733(9)[b]	89 756(9)[b]	89 703	91 351(4)[b]	91 332	94 961(9)[b]	94 972	Refs. 16, 17
35	Br VI	151 274(11)[c]	103 560(22)	103 510	105 675(22)	105 747	110 580(22)	110 661	Refs. 4, 18
36	Kr VII	170 832(9)	116 730[a]	117 257	120 080(50)	120 183	126 540(100)	126 613	Refs. 3, 19
37	Rb VIII	190 502(2)		130 951		134 642		142 868	
38	Sr IX	210 368(2)		144 609		149 141		159 477	
39	Y X	230 529(3)		158 273		163 721		176 518	
40	Zr XI	251 031(3)	171 866(8)	171 938	178 280(8)	178 372	193 992(8)	194 021	Ref. 2
41	Nb XII	271 939(4)	185 601(10)	185 619	193 084(10)	193 108	212 044(10)	212 039	Ref. 2
42	Mo XIII	293 333(4)	199 480(11)	199 347	207 980(4)	207 955	230 664(11)	230 642	Ref. 2
43	Tc XIV	315 229[d]		213 086		222 875		249 836	
44	Ru XV	337 717(11)		226 877		237 904		269 705	
45	Rh XVI	360 828(13)		240 699		253 015		290 270	
46	Pd XVII	384 660(15)		254 595		268 248		311 622	
47	Ag XVIII	409 271(17)		268 569	283 850(240)	283 600		333 814	Ref. 6
48	Cd XIX	434 696(19)		282 600		299 046		356 872	
49	In XX	461 002(21)		296 695		314 589		380 859	
50	Sn XXI	488 286(24)		310 892		330 261		405 864	
51	Sb XXII	516 569(27)		325 149		346 017		431 904	
52	Te XXIII	545 962(30)		339 515		361 899		459 084	
53	I XXIV	576 495(33)		353 954		377 870		487 430	
54	Xe XXV	608 273[d]		368 503		393 963		517 041	
55	Cs XXVI	641 313(41)		383 111		410 123		547 934	
56	Ba XXVII	675 804(46)		397 892		426 462		580 289	

[a] Not used in fitting.
[b] Uncertainties assumed 5 parts in the last-quoted place of the source wavelength.
[c] Uncertainty relative to $J = 2$ level.
[d] As interpolated in Ref. 1.

As in Ref. 9, hydrogenlike expressions were used to reduce each of the quantities further to a screening parameter. The screened hydrogenlike value for ζ is[10,11]

$$\zeta = R\alpha^2(Z - S_\zeta)^4/192 + \text{higher order}, \quad (7)$$

whereas $4s$ and $4p$ screened hydrogenlike wave functions yield a value for G_1 with an exact rational fraction

$$G_1 = (4275/262144)R(Z - S_G)/(1 + \epsilon). \quad (8)$$

Here R is the reduced-mass-corrected Rydberg constant, α is the fine-structure constant, Z is the nuclear charge, and S_i denotes the empirical screening parameters that Eqs. (7) and (8) serve to define. ϵ is an additional fitting parameter, a small correction introduced to optimize the isoelectronic regularity. The higher-order terms in Eq. (7) include additional contributions to the Dirac energy and radiative corrections that have been described in detail elsewhere.[9,11] As has been found earlier,[9] when the measured data are reduced to these effective screening parameters, their isoelectronic behavior is described very well by the ansatz

$$S_i = a_i + b_i/(Z - S_i). \quad (9)$$

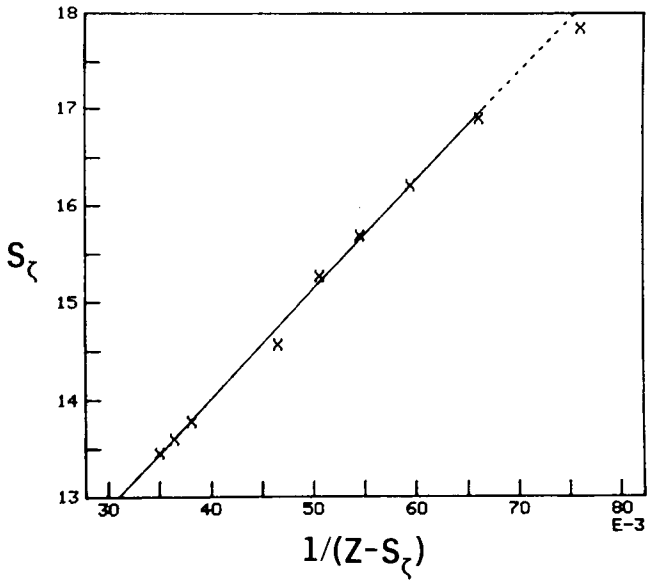

Fig. 1. Plot of the spin–orbit energy-screening parameter versus the reciprocal screened charge. X's denote the experimental data for (from right to left) Z = 31–36, 40–42. The line traces the fit described in Table 2 and is solid within the fitted region.

RESULTS

The existing measurements and their literature sources[1–4,6,12–20] are given in Table 1. The uncertainties listed in parentheses are either taken directly from the original sources or estimated from information in the original sources. Since these uncertainties determine the fitting weights, efforts were

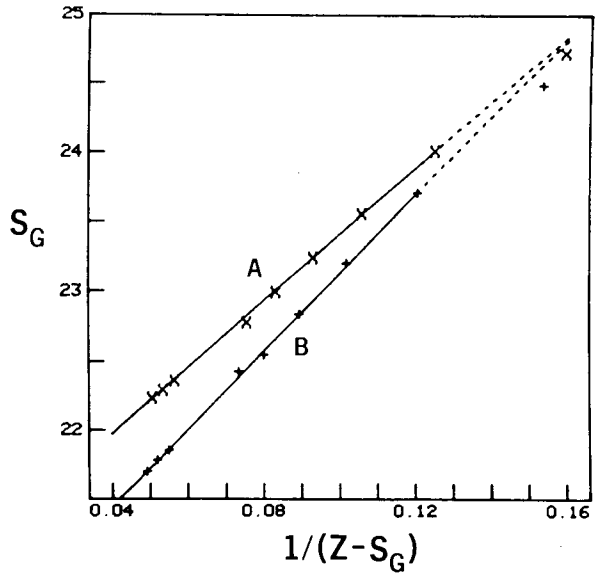

Fig. 2. Plots of the two exchange Slater energy-screening parameters versus the reciprocal screened charge. +'s denote the G_{1A} reduction of the data with $\epsilon_A = 0.004$, and ×'s denote the G_{1B} reduction of the data with $\epsilon_B = 0.042$, for (from right to left) Z = 31–36, 40–42. The line traces the fit described in Table 2 and is solid within the fitted region.

Table 2. Fitting Parameters [Eq. (9)] Least-Squares Adjusted to the Screening-Parameter Equivalents [Eqs. (1)–(8)] of the Experimental Data

Quantity i	ϵ_i	a_i	b_i
ζ	–	9.497	112.7
G_{1A}	0.004	21.00	24.06
G_{1B}	0.042	20.34	27.95

made to trace the propagation of uncertainties from source wavelength lists for each of the intervals of interest. The older references did not quote uncertainties, so (where indicated) these were estimated to be 5 parts in the last quoted figure of the determining wavelengths. Reference 1 provides a comprehensive study of the $4s4p\ ^1P_1$ excitation energy including new observations, a compilation of previous work with source references and interpolations. The adopted values and estimated uncertainties from Ref. 1 are partially reproduced in the first column of Table 1.

A reduction of this data base to the screening parameter for ζ is shown in Fig. 1, and a similar reduction to the screening parameters for G_{1A} and G_{1B} (with $\epsilon_A = 0.004$ and $\epsilon_B = 0.042$) is shown in Fig. 2. The empirical linearity of these parameterizations is apparent from these plots. The solid lines represent least-squares regressions, weighted by the reciprocal squares of the experimental uncertainties, to Eq. (8). The fitting parameters are given in Table 2. Slight curvatures usually occur at the neutral end of these screening parameter plots (neutral and singly ionized systems are subject to, e.g., perturbations from excited core configurations that diminish with increasing ionization), and only the multiply ionized data were used in the fitting.

Notice that the Kr VII point is slightly below the trend on the S_ζ and S_{GA} plots and slightly above the trend of the S_{GB} plot. All three of these discrepancies can be corrected by revising the $4s4p\ ^3P_0$ level upward by about 500 cm^{-1}. Although this is five times the quoted uncertainty, this level was determined in the beam-foil spectra of Ref. 3 from a very weak line at 614.8 Å classified as the $4s4p\ ^3P_0$–$4p^2\ ^3P_1$ transition. These interpolations would place this line at 616.7 Å, which might be concealed in the wings of the stronger $4s4p\ ^3P_2$–$4p^2\ ^3P_1$ transition at 618.67 Å.[19,20] A revision of the Kr VII $4s4p\ ^3P_0$ level to 117 230 cm^{-1} is therefore recommended. By

Table 3. Predicted Wavelengths for the Intercombination, Magnetic-Dipole, and Electric-Quadrupole Transitions (in angstroms)[a]

Z	Ion	$\lambda(^1S_1$–$^3P_1)$ Obs.	$\lambda(^1S_1$–$^3P_1)$ Pred.	$\lambda(^3P_2$–$^3P_1)$ (Pred.)	$\lambda(^3P_2$–$^3P_0)$ (Pred.)
37	Rb VIII		742.7	12 153	8 389
38	Sr IX		670.5	9 672	6 724
39	Y X		610.8	7 812	5 479
40	Zr XI	561.4(3)[b]	560.6	6 388	4 527
41	Nb XII		517.9	5 281	3 784
42	Mo XIII	480.82(1)[c]	480.9	4 407	3 194
43	Tc XIV		448.7	3 708	2 720
44	Ru XV		420.3	3 144	2 334
45	Rh XVI		395.2	2 683	2 017
46	Pd XVII		372.8	2 305	1 754
47	Ag XVIII	352.3(3)[b]	352.6	1 992	1 533
48	Cd XIX		334.4	1 729	1 346
49	In XX		317.9	1 509	1 188
50	Sn XXI		302.8	1 323	1 053
51	Sb XXII		289.0	1 164	936.7
52	Te XXIII		276.3	1 029	836.3
53	I XXIV		264.6	912.8	749.2
54	Xe XXV		253.8	812.5	673.2
55	Cs XXVI		243.8	725.6	606.7
56	Ba XXVII		234.5	650.1	548.3

[a] Wavelengths over 2000 Å are given in air.
[b] Ref. 6.
[c] Ref. 2.

similar considerations using the interpolations presented here, a revision of the excitation energies of the triplet system in Br VI was recently made.[4]

The parameterization was used together with the observed singlet energies[1] to predict triplet energies for this sequence for $Z = 32$–54, which are presented, along with the existing observations on which they are based, in Table 1. Experimental observations for the resonance transition are available up to $Z = 74$, but deviations from linearity on the G_1 screening parameter plot were noted[9] for the Be and Mg sequences as the degree of ionization approached 30. The extrapolations to high stages of ionization in Table 1 must be considered speculative, but they provide a guide to future spectroscopic studies, which will subsequently permit a refinement of these predictions. The agreement between the observations and the predictions is generally within tens of inverse centimeters (hence better than 0.1%). The measurement accuracies are often an order of magnitude more precise than this, but the screening parameterization is intended only as a predictive systematization and not as an exact description.

A tabulation of the predicted wavelengths for the $4s^2\ {}^1S_0$–$4s4p\ {}^3P_1$ intercombination line, the $M1\ 4s4p\ {}^3P_1$–${}^3P_2$ intraterm line, and the $E2\ 4s4p\ {}^3P_0$–${}^3P_2$ intraterm line is given in Table 3.

CONCLUSIONS

Screened one-electron formulas have been utilized to map the spin–orbit and exchange energies of the $4s4p$ configuration in the Zn sequence into a space where they are isoelectronically linear. This permits precise interpolations and extrapolations of the triplet energy levels relative to the singlet level for this configuration. This analysis indicates that the regularities observed earlier for the $3s3p$ configuration in the Mg sequence persist for higher homologous $nsnp$ configurations. A similar analysis is now under way for the homologous $5s5p$ Cd isoelectronic sequence, for which many new data have recently become available.[21]

ACKNOWLEDGMENTS

I am grateful to B. Denne, E. Hinnov, K. N. Huang, V. Kaufman, and J. Reader for providing me with their results before publication. This research was supported by the U.S. Department of Energy, Division of Chemical Sciences, under contract number DE-AS05-80ER10676.

REFERENCES

1. N. Acquista and J. Reader, "$4s^2\ {}^1S_0$–$4s4p\ {}^1P_1$ transitions in zinclike ions," J. Opt. Soc. Am. B **1,** 649–651 (1984).
2. U. Litzén and K. Ando, "$4s$–$4p$ transitions including intercombination lines in Zn-like Zr XI, Nb XII and Mo XIII," Phys. Lett. A **100,** 411–414 (1984).
3. E. H. Pinnington, W. Ansbacher, and J. A. Kernahan, "Energy-level and lifetime measurements for Kr VII," J. Opt. Soc. Am. B **1,** 30–33 (1984).
4. L. J. Curtis, I. Martinson, B. Denne, J. A. Leavitt, D. D. Dietrich, and S. Bashkin, "Wavelength of the $4s^2\ {}^1S_0$–$4s4p\ {}^3P_1$ intercombination line in Br VI," Phys. Lett. A **105,** 212–214 (1984).
5. M. Finkenthal, R. E. Bell, H. W. Moos, A. K. Bhatia, E. S. Marmar, J. L. Terry, and J. E. Rice, "The molybdenum spectrum emitted by a tokamak plasma in the 300–550-Å range," Phys. Lett. A **82,** 123–126 (1981).
6. B. Denne and E. Hinnov, Princeton Plasma Physics Laboratory, Princeton, New Jersey 08544 (personal communication).
7. G. A. Victor and W. R. Taylor, "Oscillator strengths and wavelengths for the copper and zinc isoelectronic sequences; $Z = 29$ to 42," Atomic Data Nucl. Data Tables **28,** 107–214 (1983).
8. K.-N. Huang, Institute of Atomic and Molecular Sciences, Academia Sinica, Taipei, Taiwan (personal communication).
9. L. J. Curtis and P. S. Ramanujam, "Isoelectronic wavelength predictions for magnetic-dipole, electric-quadrupole, and intercombination transitions in the Mg sequence," J. Opt. Soc. Am. **73,** 979–984 (1983).
10. B. Edlen, "Atomic spectra," in *Handbuch der Physik XXVII,* S. Flügge, ed. (Springer-Verlag, Berlin, 1964), pp. 80–220.
11. L. J. Curtis, "On the αZ expansion for the Dirac energy of a one-electron atom," J. Phys. B **10,** L641–L645 (1977).
12. I. Johansson and R. Contreras, "New measurements of the arc spectrum of zinc," Ark. Fys. **37,** 513–520 (1968).
13. R. A. Sawyer and R. J. Lang, "The spectrum of gallium II and the $(4s4p^2)$ configuration in gallium I and indium I," Phys. Rev. **34,** 712–719 (1929).
14. R. J. Lang, "The spark spectrum of germanium," Phys. Rev. **34,** 697–711 (1929).
15. K. R. Rao, "The third spark spectrum of arsenic (As IV)," Proc.R. Soc. London Ser. A **134,** 604–613 (1932).
16. K. R. Rao and J. S. Badami, "Investigation of the spectrum of selenium. Part I—Se IV and Se V," Proc. R. Soc. London Ser. A **131,** 154–169 (1931).
17. R. A. Sawyer and C. J. Humphreys, "The 29 and 30-electron-system spectra of arsenic and selenium," Phys. Rev. **32,** 583–592 (1928).
18. A. S. Rao and K. R. Rao, "The spectra of Br V, Br VI Br VII," Proc. Phys. Soc. London Ser. A **46,** 163–168 (1934).
19. B. C. Fawcett, B. B. Jones, and R. Wilson, "Vacuum ultraviolet spectra of multiply ionized inert gases," Proc. Phys. Soc. London Ser. **78,** 1223–1226 (1961).
20. M. Druetta and J. P. Buchet, "Beam-foil study of krypton between 400 and 800 Å," J. Opt. Soc. Am. **66,** 433–436 (1976).
21. V. Kaufman, National Bureau of Standards, Gaithersburg, Maryland 20899 (personal communication).